[1]P. Gombás, in *Encyclopedia of Physics*, edited by S. Flügge (Springer, Berlin, 1958), Vol. 36, p. 109.
[2]A. S. Kompaneets and E. S. Pavlovskii, Zh. Eksperim. i Teor. Fiz. 31, 427 (1956) [Sov. Phys. JETP 4, 328 (1957)].
[3]D. A. Kirzhnits, Zh. Eksperim. i Teor. Fiz. 32, 115 (1957) [Sov. Phys. JETP 5, 64 (1957)].
[4]G. A. Baraff and S. Borowitz, Phys. Rev. 121, 1704 (1961).
[5]G. A. Baraff, Phys. Rev. 123, 2087 (1961).
[6]H. M. Schey and J. L. Schwartz, Phys. Rev. 137, A709 (1965).
[7]R. P. Feynman, N. Metropolis, and E. Teller, Phys. Rev. 75, 1561 (1949).
[8]J. E. Enstrom, J. Chem. Phys. 46, 1213 (1967).
[9]J. C. Mason, Proc. Phys. Soc. (London) 84, 357 (1964).
[10]K. S. Viswanathan and B. N. Narahari Achar, Can. J. Phys. 42, 2332 (1964).
[11]P. Venkatarangan, Can. J. Phys. 43, 1157 (1965).
[12]T. Tietz and S. Krzeminski, Acta Phys. Acad. Sci. Hung. 27, 161 (1969).
[13]N. N. Kalitkin, Zh. Eksperim. i Teor. Fiz. 38, 1534 (1960) [Sov. Phys. JETP 11, 1106 (1960)].
[14]*Handbook of Chemistry and Physics*, 51st ed. (Chemical Rubber, Cleveland, Ohio, 1970), p. E-127.
[15]S. Kumar and A. Jain, J. Phys. Soc. Japan 28, 1046 (1970).

PHYSICAL REVIEW A VOLUME 4, NUMBER 2 AUGUST 1971

Obtaining the Optical Field Isotope Shifts of a Light Element*

Gabriel L. Epstein† and Sumner P. Davis
Department of Physics, University of California, Berkeley, California 94720
(Received 30 October 1970; revised manuscript received 1 March 1971)

The problem of obtaining field isotope shifts for light elements is discussed, and it is shown to be possible, in principle, to extract this information solely from an optical-isotope-shift experiment. We attempted such an experiment with the even-even calcium isotopes: Ca 40, 42, 44, and 48. We found that an accuracy of $\sim 10^{-5}$ cm^{-1} in the measurements would be required to effect the separation. Lacking that accuracy, we considered the conditions under which optical-isotope-shift measurements may be combined with those of other isotope-shift experiments. The even-even calcium isotopes fulfill these conditions, allowing the desired separation of optical mass- and field-effect isotope shifts to be accomplished by drawing on the results of muonic x-ray and electron-scattering experiments. The optical field-effect shifts thereby found are shown to corroborate the picture of the calcium nuclei derived from those experiments. A correlation between the relative isotope shift and the binding energy per nucleon, proposed by Gerstenkorn, is shown to apply to the calcium isotope shifts.

Isotope shifts in atomic spectrum lines of heavy elements are attributed mainly to isotopic differences in the nuclear charge distribution.[1] The shifts in a single line for a series of isotope pairs show the changes in the mean square radius of the nuclear ground-state charge distribution. Since there appear to be sharp changes in intrinsic nuclear shapes at magic neutron numbers,[2] it is particularly valuable to make such measurements on a series of nuclei containing a magic-number nucleus.

The same consideration applies to light elements, but both the experimental and interpretational problems are more difficult. For these elements the shifts due to mass differences in the nuclei cannot be neglected, and it is exceedingly difficult to separate the mass- and field-effect shifts. In fact, these can be opposite in sign, resulting in a net shift smaller than the Doppler widths of the spectral lines. However, it seems worthwhile to attempt this separation for calcium since the series of even-even isotopes both starts and ends with a doubly magic nucleus. Further, since the behavior of the mean square radius of the nuclear charge distribution of the calcium isotopes is known (from muonic x-ray and electron-scattering experiments), we can determine when we have achieved a valid separation of the optical mass- and field-effect shifts.

Interest in calcium was spurred in 1963 when a measurement[3] of the $2p$-$1s$ muonic x-ray transition suggested that the addition of four neutrons to the Ca 40 nucleus results in a smaller proton volume—contrary to the widely held assumption (at that time) that the nuclear charge radius is proportional to $A^{1/3}$. Although later experiments[4–6] have shown that Ca 44 does indeed have the larger charge radius, it is not so large as predicted from the $A^{1/3}$ law.

I. DEPENDENCE OF ISOTOPE SHIFTS ON ATOMIC AND NUCLEAR PROPERTIES

In isotope-shift calculations for hydrogenic atoms, the fact that the nucleus has finite mass is easily treated by use of the reduced electron mass μ. The result is that $E(\mu)$, the true energy eigenvalue, is equal to $(\mu/m_e)E(m_e)$, the energy eigen-

value for an infinite mass nucleus. The atomic terms of a heavier isotope are lower in energy (more negative) than the corresponding terms of a lighter isotope. Each spectrum line is shifted by

$$\Delta\sigma = (m_e/m_p)\,[\Delta A/A(A+\Delta A)]\sigma \text{ cm}^{-1}\,, \qquad (1)$$

where m_e and m_p are the electron and proton masses, A and $(A+\Delta A)$ the mass numbers of the isotopes, and σ the wave number of the spectrum line.

For other spectra calculation of the mass-effect shift is much more complicated and depends upon knowledge of accurate electron wave functions and how they fit together to form the total atomic wave function.[7] Hughes and Eckart[8] showed that, neglecting spin-orbit coupling, the effect may be expressed as the sum of the normal-mass shift [Eq. (1)] and a specific-mass shift arising from electron-electron correlation. The specific-mass shift varies inversely as the square of the nuclear mass; however, it also depends on the number of atomic electrons, and there is evidence[9] that it is not negligible for intermediate elements. Further, while the normal-mass shift is to shorter wavelengths as the nuclear mass increases, the specific-mass shift can be to longer or shorter wavelengths. In any case, the specific-mass shift in a spectrum line can be expressed as the product of a nuclear and an atomic factor:

$$\Delta\sigma\,(\text{specific mass}) = [\Delta A/A(A+\Delta A)]S_a\,. \qquad (2)$$

The subscript a on the mass-shift coefficient S_a refers to the spectrum line involved.

Those electrons that penetrate a nuclear charge distribution of finite extent are bound less strongly than they would be to an idealized point nucleus. If it is assumed that the heavier of two isotopes has the larger charge volume, then its energy levels are shifted up further toward the ionization limit. Since s electrons have the greatest penetration of the nucleus, an optical transition in which the number of s electrons is increased is shifted to longer wavelengths as neutrons are added to the nucleus (e.g., the $4s4p\ ^1P_1$-$4s^2\ ^1S_0$ 4227-Å Ca I transition).

Calculations of the field effect, both with the perturbation approach[10] and with the more accurate boundary matching technique,[11] show that

$$\Delta\sigma(\text{volume}) = E_a C\,(Z, \delta\langle r^{2\gamma}\rangle)_{A_i, A_j}\,. \qquad (3)$$

E_a depends on the variation of the sum of all the electron wave functions at the nucleus during the transition. It is usually assumed to be completely determined by the optical electron in its s state, the variation of the wave functions of the electron core being neglected.[12] It does not vary with neutron number. The isotope-shift constant C characterizes the difference in the nuclear charge distributions of the pair of isotopes A_i, A_j and is proportional to $\delta\langle r^{2\gamma}\rangle$, where

$$\langle r^{2\gamma}\rangle \equiv \int \rho_N(r) r^{2\gamma+2}\,dr, \quad \gamma \equiv (1-\alpha^2 Z^2)^{1/2}\,.$$

The proportionality between $\delta\langle r^{2\gamma}\rangle$ and C depends upon the assumptions of nuclear compressibility[13] and deformation.[14] For lighter elements $\gamma \to 1$, and the field shift becomes proportional to the change in mean square radius from one isotope to another. For calcium $\gamma = 0.989$.

II. SEPARATION OF MASS AND FIELD ISOTOPE SHIFTS

From Eqs. (1)—(3) the observed shift in a spectrum line (index a) for the pair of isotopes with mass numbers A_i and A_{i+1} can be written

$$\Delta\sigma_{ia} = C_i E_a + m_i S_a\,, \qquad (4)$$

where $m_i \equiv A/A(A+\Delta A) = (A_{i+1}-A_i)/A_iA_{i+1}$ and we now choose S_a to include both normal- and specific-mass shifts.

In spite of a common belief to the contrary, Eq. (4) allows the separation of mass and field isotope shifts, at least in principle. Suppose we can measure the shifts in two spectrum lines a and b for three isotope pairs A_1A_2, A_2A_3, and A_3A_4, and write Eq. (4) for each of these measurements. Combining the equations for the isotope pairs A_1A_2 and A_2A_3 and then rearranging, we have

$$S_b = \frac{\Delta\sigma_{1b}\Delta\sigma_{2a} - \Delta\sigma_{1a}\Delta\sigma_{2b}}{m_1\Delta\sigma_{2a} - m_2\Delta\sigma_{1a}} - \left(\frac{m_2\Delta\sigma_{1b} - m_1\Delta\sigma_{2b}}{m_1\Delta\sigma_{2a} - m_2\Delta\sigma_{1a}}\right)S_a\,. \qquad (5)$$

Applying the same steps to the isotope pairs A_1A_2 and A_3A_4 and solving for the total mass-shift coefficient, we have

$$S_a = \frac{\left(\dfrac{\Delta\sigma_{1b}\Delta\sigma_{2a} - \Delta\sigma_{1a}\Delta\sigma_{2b}}{m_1\Delta\sigma_{2b} - m_2\Delta\sigma_{1a}} - \dfrac{\Delta\sigma_{1b}\Delta\sigma_{3a} - \Delta\sigma_{1a}\Delta\sigma_{3b}}{m_1\Delta\sigma_{3a} - m_3\Delta\sigma_{1a}}\right)}{\left(\dfrac{m_3\Delta\sigma_{1b} - m_1\Delta\sigma_{3b}}{m_1\Delta\sigma_{3a} - m_3\Delta\sigma_{1a}} - \dfrac{m_2\Delta\sigma_{1b} - m_1\Delta\sigma_{2b}}{m_1\Delta\sigma_{2a} - m_2\Delta\sigma_{1a}}\right)}\,. \qquad (6)$$

We can therefore determine this coefficient from the known factors m_i and the experimentally measured isotope shifts for three pairs of isotopes and two spectrum lines. It should be noted that because of the many arithmetical operations in Eq. (6) with numbers of nearly equal sizes, any uncertainties in experimental measurements are greatly magnified. Finally, the isotope-shift constant C, and hence $\delta\langle r^{2\gamma}\rangle$, can be determined from Eqs. (3) and (4), subject to evaluation of the factor E_a.

For calcium, there is another means by which $\delta\langle r^{2\gamma}\rangle$ can be deduced: from data obtained from muonic x rays, atomic K x rays, and electron-scattering experiments. Bruch *et al.*[15] point out that the quantities

$$\zeta_i \equiv \Delta\sigma_{ia}/m_i = (C_i/m_i)E_a + S_a\,,$$
$$\xi_i \equiv \Delta\sigma_{ib}/m_i = (C_i/m_i)E_b + S_b \qquad (7)$$

are linearly related by

$$\zeta_i = (E_a/E_b)\xi_i + [S_a - (E_a/E_b)S_b] . \quad (8)$$

Further, if the mass shifts for a particular transition (e.g., that one indexed by b) should happen to be zero, then using the shifts for this transition as ξ abscissas with those for another transition as ζ ordinates will give the total mass-shift coefficient S_a for that transition as the ζ intercept.

Muonic x-ray measurements yield nuclear volume isotope shifts directly. [15] A beam of muons is directed into an isotopically pure sample; some are captured in outer Bohr orbits and cascade toward the nucleus. The muonic x ray emitted during the $2p$-$1s$ transition is measured, and the experiment is repeated with another isotope as the target. In low quantum states "the μ-meson wave function is not perturbed by the atomic electrons" and the system can be treated as hydrogenic. [16] Hence, correcting the experimental shifts for the exactly calculable normal-mass shifts yields quantities that can be attributed solely to changes in the nuclear charge distribution.

Similarly, when high-energy electrons (hundreds of MeV) are used as a probe, they can be treated as though scattered only by the nuclei and unaffected by the atomic electrons in the target. [17] Phenomenological charge distributions are used to predict scattering behavior, and two nuclear parameters (half-density charge radius and skin thickness) are varied to give the best fit. [18] A more direct route to the isotopic changes in $r_{0.5}$ and skin thickness is to measure ratios of cross sections and compute a difference function that emphasizes the angular positions of the cross sections's maxima and minima. [19]

Atomic K x rays are valuable nuclear probes that have received increasing attention in the last few years. [20–22] Because the K-level electron is so much closer to the nucleus than the optical electron, both the energy of the transition and the relative energy shifts $\delta E/E$ are greater. A more significant advantage of the K x-ray technique is that the specific-mass shift can be reliably evaluated, [23] thus allowing isolation of the field-effect shift from the measured total isotope shift.

The volume shifts derived from a nonoptical-isotope-shift experiment can be used to obtain S_a for an optical transition in the following manner. We assume that we can write the field, or volume, shift from the nonoptical measurement as

$$\delta E_i = \sum_{n=1}^{\infty} E_{ni}\, \delta\langle r^{2n}\rangle . \quad (9)$$

Then we have

$$\zeta_i = \left(\frac{C_i}{m_i}\right) E_a + S_a , \quad \chi_i = \sum_{n=1}^{\infty} \frac{E_{ni}}{m_i}\, \delta\langle r^{2n}\rangle \quad (S_b = 0), \quad (10)$$

$$\zeta_1 = \left[E_a C_i \Big/ \sum_{n=1}^{\infty} E_{ni}\delta\langle r^{2n}\rangle\right]\chi_i + S_a , \quad (11)$$

where the index i refers to the isotope pair for which the measurement is made. If the term in brackets is independent of neutron number, then a plot of ζ_i vs χ_i is linear, and the total mass-shift coefficient S_a of the optical transition is immediately found as the ζ intercept.

The numerator of the bracketed term depends on neutron number only through the factor $\delta\langle r^{2\gamma}\rangle \cong \delta\langle r^2\rangle$. Thus, for this term to be independent of the isotope pair (index i), terms of Eq. (9) involving moments of the nuclear charge distribution higher than $\langle r^2\rangle$ must be small enough to be neglected. In the case of K x rays, Seltzer[24] has calculated that $E_2/E_1 \lesssim 10^{-3}$ so that our plot should be linear to a good approximation. For muonic x rays, moments other than $\langle r^2\rangle$ are involved as demonstrated in a recent study by Ford and Wills. [25] However, it has been pointed out that taking the ratio of the volume shifts derived from muonic x-ray measurements cancels to a good approximation the influence of the higher moments of the nuclear charge distribution. [26] That this is effectively what is done for the ζ, χ plot can be seen by writing the slope evaluated at two isotope pairs j and k and equating the two expressions.

Bruch *et al.* [27] have used this type of plot for a number of light- and intermediate-weight elements, and for pairs of isotopes with even proton and neutron numbers the plots are linear to within the experimental errors. However, as they point out, points for isotope pairs including an odd isotope show marked deviations. This suggests that the odd neutron distorts the nuclear charge distribution enough so that the slope in Eq. (11) changes. This can come about either because terms higher than the first in Eq. (9) can no longer be neglected or because the nonoptical probe (muon or K-level electron) interacts disproportionately more with the deformation component of the mean square charge radius than does the optical electron.

Once S_a is obtained for a particular optical transition, the quantities $C_i E_a$ (the field-effect isotope shifts) may be found from Eq. (4) for the whole series of isotope pairs. To get the isotope-shift constant C_i, and hence $\delta\langle r^{2\gamma}\rangle$, E_a must be evaluated for the transition studied. Since this can be done with an accuracy of only 20%, [28,29] it is usual to consider the relative isotope shifts

$$\Delta\sigma(\mathrm{rel}) \equiv \frac{E_b C(Z, \delta\langle r^{2\gamma}\rangle)\big|_{A_i}^{A_{i+1}}}{E_b C(Z, \delta\langle r^{2\gamma}\rangle)\big|_{A_k}^{A_{k+1}}} \quad (i = 1, \ldots, n-1) , \quad (12)$$

$$\Delta\sigma(\mathrm{rel}) = \frac{\delta\langle r^{2\gamma}\rangle\big|_{A_i}^{A_{i+1}}}{\delta\langle r^{2\gamma}\rangle\big|_{A_k}^{A_{k+1}}} \quad (i = 1, \ldots, n-1) . \quad (13)$$

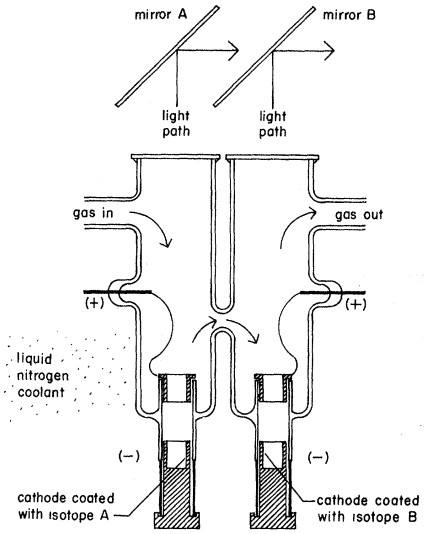

FIG. 1. Double hollow cathode lamp used for sequential scanning of the Ca I resonance line at 4227 Å with separated isotopes. A discharge was struck in cathode *B* and a scan record built up for the line from isotope *B*; then mirror *B* was removed and the same done for the line from isotope *A*. Mirrors *A* and *B* were adjusted until the light from the two cathodes illuminated the interferometer in the same way.

III. EXPERIMENTAL ASPECTS

The first spectrum line chosen for investigation was the Ca I resonance line at 4227 Å ($4s4p\ ^1P_1$-$4s^2\ ^1S_0$). The largest isotope shift in this line, between isotopes 40 and 48, [30] is about 0.050 cm^{-1}, while we felt the shifts must be measured to about 0.0001 cm^{-1} if Eq. (6) was to give a number with a meaningful error. It seemed out of the question to make a light source that emitted the resonance line with a width even 100 times this figure, so we settled on making a stable and reproducible source with as small a linewidth as reasonably possible, obtaining well-separated isotopes, and observing them separately and alternately.

An atomic-beam light source gives the narrowest linewidths but requires too much material to be used with separated isotopes. A liquid-helium hollow cathode has an effective temperature[31] of about 40 K with a corresponding linewidth of 0.017 cm^{-1} for the calcium resonance line; a liquid-nitrogen-cooled hollow cathode has a temperature of about 110 K with a linewidth of 0.026 cm^{-1}. We chose the latter because of its ease of operation and because the narrower line from the helium-cooled source would not change the final accuracy appreciably, as will become clear.

The double hollow cathode lamp shown in Fig. 1 was developed to allow sequential scanning of the same spectral line for two separated isotopes. Each anode-cathode pair was as much alike as possible, and the common housing ensured the same carrier gas pressure in each. Several methods were tried for coating the cathodes with the separated isotopes. A coating prepared from a slurry of $CaCO_3$ gave 10–50 times more intensity in the resonance line than one made from deliquescent $CaCl_2 \cdot H_2O$. The linewidths achieved with this source are shown in Fig. 2. The instrumental linewidth of about 0.025 cm^{-1} gives, when deconvolved from the recorded linewidths, a minimum emission linewidth of about 0.025 cm^{-1}, in agreement with Chantrel's results (see Ref. 31). The lamp gave good intensity for over 60 h of operation with a charge of 5 mg of the separated isotopes.

A scanning Fabry-Perot interferometer was used together with a Nuclear Data Co. Enhancetron signal averager to achieve the high resolution and throughput necessary for observing sharp lines from a weak light source. The effective linewidth was about 0.050 cm^{-1}, so the free spectral range was chosen to be 0.100 cm^{-1}, equivalent to a plate separation of 5 cm. The plates, which were flat to $\lambda/70$ at 4358 Å, were coated with a five-layer dielectric coating which gave a reflectance of about

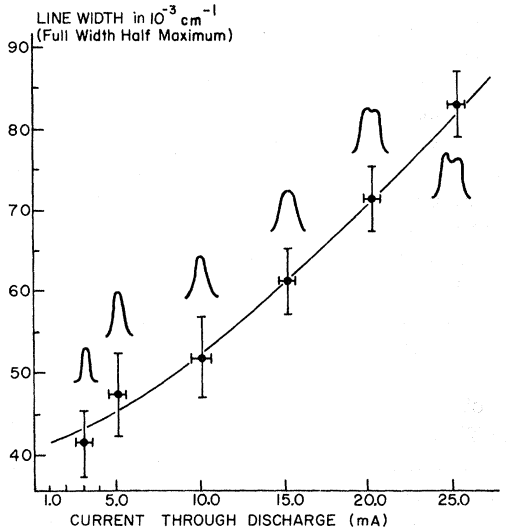

FIG. 2. Instrumental linewidth (result of interferometer and the electronics) increased the lamp linewidth (convolution of Doppler, collision, and natural linewidths) by about 0.025 cm^{-1}. The large variation in linewidth (± 0.004 cm^{-1}) seemed to arise from variation of carrier gas pressure in the hollow cathode and from the length of time the discharge had been maintained when the measurement was made. The linewidth was generally greater after an hour of running the lamp while each measurement of linewidth took about 5 or 10 min. The line shapes obtained are shown near each point; self-reversal of the resonance line occurred for currents of 20 mA and over.

89%[32] at 4227 Å.

The plates were driven (scanned) by three stacks of piezoelectric disks; each stack consisted of six clevite disks cemented together with conductive Epoxy, connected in series mechanically but in parallel electrically. The disks were selected for equal voltage to mechanical expansion to ensure that the interferometer plates remained parallel during a scan, and so that equal voltage changes corresponded to equal changes in the optical path length through the interferometer. A change of 400 V was sufficient to change the thickness by about 0.5 μ, or 2.5 free spectral ranges at 4227 Å. The piezoelectric stacks were driven by the triangular sweep voltage obtained from the Enhancetron channel-advance voltage as passed through a dc operational amplifier. It was monitored with a Tektronix 547 oscilloscope and found to be linear to within 1%.

To isolate the 4227-Å line of calcium an interference filter centered at 4230 Å was used. It had a full bandwidth at half-maximum of 10 Å and a transmission of 29% at the resonance line. (The filter was purchased from Thin Film Products, Cambridge, Mass.) The Fabry-Perot rings were focused on a pinhole of 7-μ diam by means of a projection lens of 330-mm focal length. The scan signal was detected with a IP28 photomultiplier, specially selected for low noise output and placed behind the pinhole.

The detector output was fed into a Nuclear Data Co. 1024-channel Enhancetron, for the purposes of signal averaging. The 1024 channels were split into two groups of 512, each group being used to store data from a single isotope. Since the triangular channel-advance voltage was used to control the Fabry-Perot interferometer sweep, a direct correspondence was established between channel number and interferometer spacing (wave number being recorded). Thus, a spectrum line could be scanned (and the scan stored) for one isotope at a time and the shift in the line (between isotopes) found as the shift of one scan relative to the other. To be sure that the correspondence between channel number and interferometer spacing (wave number sampled) was the same for both groups of 512 channels, the starting voltage of the sweep was monitored with a Tektronix storage oscilloscope used with a voltage off-set plug-in. It was found that the starting voltage for each bank of channels was constant to better than 1 in 400 V. This variation broadened the recorded linewidth by about 0.0007 cm^{-1}.

Between the two channel banks, the difference in the average starting voltage was 0.5 V and statistically variable, resulting in a possible shift of 0.0003 cm^{-1} between corresponding channels of the channel banks. To determine if the lag between the application of the scan voltage to the piezoelectric stacks and the motion of the interferometer plate introduced any shifts, various scanning periods (between 1 and 16 sec) were used. No differences in the measured isotope shifts were noted for the different scanning periods, although the lines were broadened at the faster scan speeds.

In the actual measurements of the isotope shifts, light from one cathode was directed toward the Fabry-Perot interferometer as indicated in Fig. 3. It was chopped at 600 Hz in the focal plane of lens L_1, and after passing through the interferometer the modulated light was detected with the IP28 photomultiplier. After rectification in a PAR HR8 phase-sensitive detector, the signal was fed into one bank (512 channels) of the Enhancetron where, for each channel, it was integrated over 27 msec, digitized, and stored in a core memory. As soon as a channel was one-third full, the Enhancetron was switched to the second bank and light from the other hollow cathode was sent through the apparatus. When a channel in this second bank became one-third full, a switch was made back to the initial channel bank

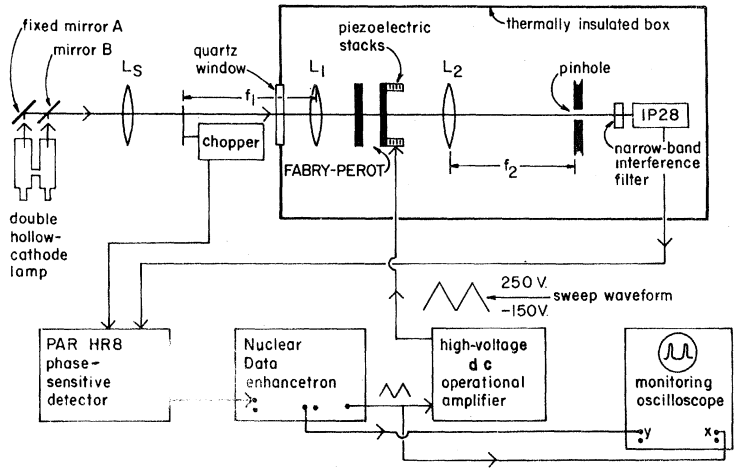

FIG. 3. Schematic diagram of experiment (see text for explanation).

and hollow cathode. This switching procedure was repeated at both two-thirds points and at the first full point, a complete scan record being built up in about 20 min.

The time-averaging property of the Enhancetron improved the signal-to-noise ratio by about 13 to a final value of better than 100/1. Although the phase-sensitive detector was redundant from the point of view of final signal to noise, it was invaluable in touching up the interferometer just before taking a scan record. The zero-voltage spacing of the Fabry-Perot interferometer had to be adjusted so that at least two free spectral ranges could be scanned for each isotope. Also, the positioning of the cathodes occasionally had to be adjusted. Use of the triangular sweep allowed the interferometer to be scanned through the spectral orders in both directions, greatly reducing the effects of source fluctuations and drifting of the electronics.

The ambient temperature varied randomly with a period of minutes so that this effect was not averaged out. To mitigate this problem a plywood housing covered with glass wool and aluminum foil was placed around the interferometer. Use of the plywood box and the technique of switching back and forth between cathode-channel bank pairs proved to be quite effective. During a series of test scans the temperature was allowed to increase from 15 to 22 °C, equivalent to scanning the interferometer by 3.5 orders. Yet the averaged isotope shift obtained from these scans was within 0.0006 cm^{-1} of the averaged shift from temperature-stable runs.

To calibrate the apparatus a series of runs was made with each hollow cathode coated with calcium 40. Light from the front cathode gave a consistently lower wave-number reading than that from the rear cathode, the magnitude of this artifical shift varying with the hollow cathode current. Since the two anode-cathode pairs were made as much alike as possible, it is felt that this shift, never more than -0.58×10^{-3} cm^{-1}, was caused by small differences in the way light from each cathode illuminated the interferometer. This is consistent with the decrease in the shift at higher hollow cathode currents. At such currents (greater than 10 mA), the plasma completely filled the cathode bore providing a larger, more uniform light source. Each isotope-shift measurement was corrected consistent with the current used when the data for that measurement were taken. The experimental measurements are shown in Table I, and a typical scan record is shown in Fig. 4.

IV. ANALYSIS OF MEASURED ISOTOPE SHIFTS

If indeed the isotope shift of a particular spectrum line can be expressed by Eq. (4) (as the sum of mass- and field-effect shifts), then the quantity $\zeta_i \equiv \Delta\sigma_{ia}/m_i$ of spectrum line a should be a linear function of the quantity $\xi_i \equiv \Delta\sigma_{ib}/m_i$ of spectrum line b. This is shown in Fig. 5 for Ca I 4227 Å ($4s4p\,^1P_1$-$4s^2\,^1S_0$) (measurements herein described) and Ca II 3933 Å ($4p\,^2P_{3/2}-4s\,^2S_{1/2}$) (measurements by Bruch *et al.*[15] with a pressure scanned Fabry-Perot interferometer). That a straight-line graph is obtained with these two spectral lines underscores the fact that it is the joint nuclear properties (for a pair of isotopes) that vary from point to point—not the atomic factors. The slope of the line [Eq. (8)] gives the ratio of the electronic factors for the two s-electron atomic terms involved: $4s^2\,^1S_0$ and $4s\,^2S_{1/2}$. From the definition of E_a [see

TABLE I. Isotope shifts for the 4227-Å calcium resonance line. Runs with Ca 40 used in both cathodes were made to calibrate the apparatus. Each of the other runs was then corrected according to the hollow cathode current used for that run (column 6). All shifts are given in 10^{-3} cm^{-1}.

Isotope pair	Free spectral range (10^{-3} cm^{-1})	No. of scans	Cathode current (mA)	Shifts (10^{-3} cm^{-1})	Corrected shifts (10^{-3} cm^{-1})	Average shifts (10^{-3} cm^{-1})
40, 42	107.5 ± 0.0011	15	3	12.17 ± 0.10	12.75 ± 0.3	12.8 ± 0.3
	97.9 ± 0.015	20	3	12.22 ± 0.17	12.80 ± 0.3	
40, 44	107.5 ± 0.01	20	6	24.00 ± 0.09	24.40 ± 0.1	24.9 ± 0.2
	100.3 ± 0.0002	20	6	25.10 ± 0.09	25.50 ± 0.1	
	98.43 ± 0.05	10	10	24.60 ± 0.20	24.79 ± 0.2	
	98.43 ± 0.05	10	5	24.34 ± 0.20	24.81 ± 0.2	
40, 48	100.3 ± 0.002	20	12	50.27 ± 0.15	50.42 ± 0.3	50.5 ± 0.4
	122.0 ± 0.10	20	14	50.39 ± 0.30	50.48 ± 0.4	
40, 40	98.4 ± 0.05	25	3	−0.58 ± 0.13		
		10	5	−0.47 ± 0.07		
		10	10	−0.19 ± 0.15		
		9	15	−0.05 ± 0.04		
		9	20	−0.10 ± 0.06		
		6	25	−0.15 ± 0.15		

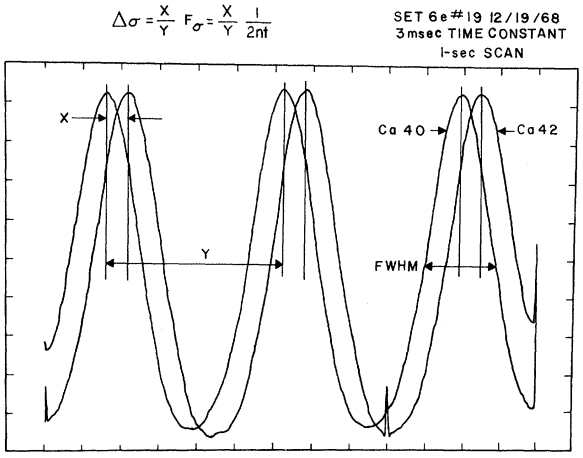

FIG. 4. Scan record showing wave number shift in Ca I resonance line (4227 Å) between isotopes Ca 40 and Ca 42. The distance between the interferometer plates was 5.1079 ± 0.008 cm, giving a free spectral range of 0.09789 cm^{-1}. The isotope shift was found as $\Delta\sigma = (X/Y)F_\sigma = (X/Y)0.09789$ cm^{-1}. The linewidth (FWHM) for this scan record was 0.0392 cm^{-1}.

Eq. (3)] and Eqs. (2) and (3) of Crawford and Schawlow,[33] we have

$$\frac{E_{3933\text{Å}}}{E_{4227\text{Å}}} = \frac{\psi^2(^2S_{1/2})|_0}{\psi^2(^1S_0)|_0} \simeq \frac{T'^{3/2}/Z_0'}{T^{3/2}/Z_0} = \frac{95248\ \text{cm}^{-1}}{49305\ \text{cm}^{-1}}\left(\frac{1}{2}\right) = 1.36\ . \tag{14}$$

This figure compares quite well with the value 1.34 from Fig. 5.

As explained before, if the shifts in two spectral lines are measured for three pairs of isotopes, the total mass-shift coefficient for one of the lines, S_a, can be calculated with Eq. (6). Unfortunately, the relative uncertainty achieved in the isotope-shift measurements, about 2%, is still too great to permit meaningful evaluation of S_a. The value obtained is -10.7 ± 78.4 cm^{-1}. Part of the difficulty stems from the fact that the measurements on the Ca II (3933 Å) line (taken from a graph in Bruch *et al.*[15]) were for different isotope pairs than the measurements described here. Measurement of the isotope shifts in the two lines for the same pairs of isotopes would eliminate recalculation and the consequent increase in inaccuracy. But basically the experimental uncertainty must be reduced by an order of magnitude, in both their measurements and ours, to 2×10^{-5} cm^{-1} to achieve meaningful calculation of S_a.

Plotting the optical isotope shifts for Ca I 4227 Å against data from electron-scattering and muonic x-ray experiments yields Fig. 6. Least-squares fitting gives the two lines shown, while weighting the two ζ intercepts in accord with their uncertainties gives the total mass-shift coefficient $S_{4227\text{Å}} = 12.0 \pm 0.3$ cm^{-1}. Table II shows the various mass- and field-effect isotope shifts for the even-even calcium isotopes. The last column gives those values of the field-effect shifts expected on the assumption of a uniform incompressible spherical nuclear charge with radius proportional to $A^{1/3}$. First-order perturbation theory gives

$$\frac{\delta(\Delta E)}{hc} = \Delta\sigma = -\frac{32\pi^2(\gamma+1)Ze^2\psi_{ns}^2(0)}{(2\gamma+1)\Gamma^2(2\gamma+1)hc}\left(\frac{2Z}{a_H}\right)^{2\gamma-2}\delta\langle r^{2\gamma}\rangle\ , \tag{15}$$

where

$$\delta\langle r^{2\gamma}\rangle \equiv \delta\int_0^r r^{2\gamma+2}\rho_N(r)\,r\,dr$$

and the normalization is such that $\int_0^r \rho_N(r)r^2\,dr = 1$. The probability density for the s electron in the neighborhood of a point charge is given by Racah[34]

$$P(r) = \frac{2(\gamma+1)}{\Gamma^2(2\gamma+1)}\psi_{ns}^2(0)\left(\frac{2Zr}{a_H}\right)^{2\gamma-2}\ , \quad \gamma \equiv (1-\alpha^2Z^2)^{1/2}\ . \tag{16}$$

The square of the s-electron wave function is obtained with the formula

$$\psi_{ns}^2(0) = \frac{Z_i Z_0^2}{\pi a_H^3 n^{*3}}\left(1 - \frac{d\Delta}{dn^*}\right)\ , \tag{17}$$

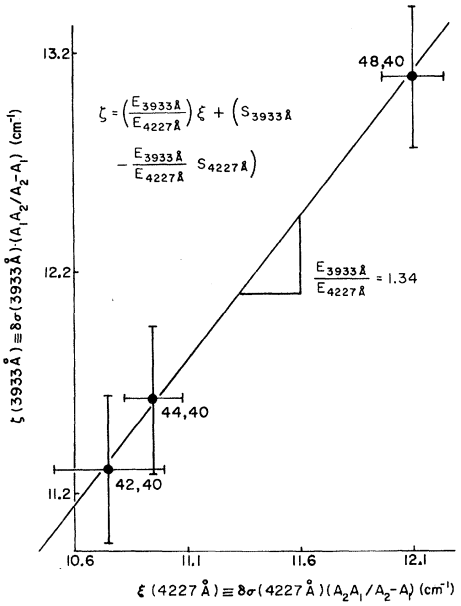

FIG. 5. ξ, ζ plot of optical isotope shifts for calcium. The ordinate shows the data of Bruch *et al.* for the Ca II line at 3933 Å (see Ref. 15). The abscissa gives the data from the current experiment on the Ca I line at 4227 Å. The experimental uncertainty of Bruch *et al.* is half that indicated; however, different isotope pairs were used in the two experiments, and calculation of the shifts for the appropriate pairs increases the uncertainties.

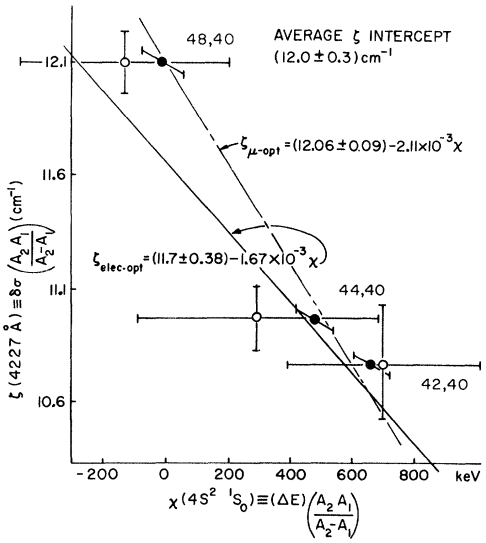

FIG. 6. Data for the muonic x-ray and electron-scattering experiments are taken from Ref. 15; prime sources of the data are given in that paper. The two equations were obtained by least-squares fitting, and the ζ intercepts, weighted according to their uncertainties, were averaged to give $S(4227\ \text{Å}) = 12.0 \pm 0.3\ \text{cm}^{-1}$.

as developed by Goudsmit[35] and Fermi and Segrè.[36] Z_i is the effective nuclear charge in the inner regions of the atom (equal to Z for the s electron), Z_0 is the charge the optical electron sees in the outer regions, n^* is the effective quantum number, and Δ is the quantum defect. The factor $(1 - d\Delta/dn^*)$ was evaluated from the $4s$, ns series of term values as outlined by Crawford and Schawlow.[33] For calcium

$$\Delta\sigma(\text{volume}) = -(1.81\times10^{23})\delta R^{2\gamma}\ \text{cm}^{-1}\ ,$$
$$R \equiv (1.25\times10^{-13})A^{1/3}\ \text{fm}\ . \qquad (18)$$

V. EVEN-EVEN CALCIUM ISOTOPES

Taking $\langle r^{2\gamma}\rangle$ as essentially the mean square charge radius, the greatest increase in nuclear radius occurs between Ca 40 and Ca 42. The increase from Ca 42 to Ca 44 is appreciably less, while from Ca 44 to Ca 48 there is a decrease in radius. The fact that the volume shift between Ca 40 and Ca 48 (Table II) is positive means that Ca 48 has the smaller nuclear charge radius. This behavior is consistent with that deduced from muonic x-ray and electron-scattering data.

Gibson and Van Oostrum[37] used a simple nuclear shell model with a Woods-Saxon potential to produce nuclear charge densities that lead to electron-scattering cross sections in agreement with experiment as well as with phenomenological analyses. The rms radii they calculate for the nuclear ground-state calcium nuclei are

$$r_{40} = 3.44\ \text{fm}\ ,\quad r_{44} = 3.46\ \text{fm}\ ,\quad r_{48} = 3.41\ \text{fm}\ .$$

These values imply [see Eq. (13)] a relative isotope shift ratio $(r_{44} - r_{40})/(r_{48} - r_{44}) = -0.55$. Our results give -0.83 for this ratio while Bruch *et al.*[38] get -0.89 using the Ca II line 3933 Å.

Both the first and last members of the series (Ca 40 and Ca 48) are doubly magic and are thus expected to be spherical. Whether or not the other calcium nuclei are spherical cannot be decided on the basis of the optical-isotope-shift experiment. Gibson and Van Oostrum[37] assume a spherical charge distribution of the form

$$\rho_N(r) = \rho_0(1 - wr^2/c^2)(1 + e^{(r^n - c^n)/z^n})^{-1}\ ,$$

where $n = 1$ (Fermi) and $n = 2$ (modified Gaussian) are usually used. They attribute the decrease in rms radius between Ca 44 and Ca 48 to a sharpening of the nuclear charge surface, rather than to a deformed Ca 44 nucleus.

VI. NUCLEAR BINDING ENERGY AND FIELD-EFFECT ISOTOPE SHIFTS

While experimental values of field-effect isotope shifts are in general smaller than the calculated values,[39] those for calcium seem particularly small and the negative shift between Ca 44 and Ca 48 is quite striking. Aside from calcium, few elements exhibit negative isotope shifts, and those reported

TABLE II. Isotope shifts in Ca I (4227 Å). All shifts are given in 10^{-3} cm^{-1}. The volume shifts are calculated as $\Delta\sigma_{\text{expt}} - [(A_2 - A_1)/A_1A_2]S_{4227\,\text{Å}}$, where the total mass-shift coefficient is 12.06 ± 0.3 cm^{-1} from Fig. 6. The normal-mass shifts are exactly calculable [Eq. (1)], whence the specific-mass shifts are $\Delta\sigma_{sp} = \Delta\sigma_m - \Delta\sigma_n = [(A_2 - A_1)/A_1A_2] \times S_{4227\,\text{Å}}$. J. Bauche (private communication) has recently calculated the specific-mass shift in the Hartree-Fock approximation. His value for $\Delta\sigma(4s4p\ ^1P_1 - 4s^2\ ^1S_0) = -12.2 \times 10^{-3}$ cm^{-1} for the pair Ca 40-Ca 42.

Isotope pair	Total isotope shift $\Delta\sigma$ (10^{-3} cm^{-1})	Total mass shift $\Delta\sigma_m$ (10^{-3} cm^{-1})	Normal shift $\Delta\sigma_n$ (10^{-3} cm^{-1})	Specific mass shift $\Delta\sigma$ (10^{-3} cm^{-1})	Volume shift $\Delta\sigma_v$ (10^{-3} cm^{-1})	Theoretical volume shifts $\Delta\sigma$ (10^{-3} cm^{-1})
40, 42	12.78 ± 0.3	14.28 ± 0.35	$+15.33$	-1.1 ± 0.4	-1.5 ± 0.7	-2.4
40, 44	24.88 ± 0.2	27.27 ± 0.68	$+29.27$	-2.0 ± 0.7	-2.4 ± 0.9	-4.5
40, 48	50.48 ± 0.4	50.00 ± 1.25	$+53.67$	-3.7 ± 1.3	$+0.5 \pm 1.6$	-8.4

involve nuclei with magic neutron numbers. Recently Gerstenkorn[40] showed that a simple correlation seems to exist between relative isotope shifts and the binding energy per nucleon—in the vicinity of certain magic neutron numbers. He gives the relationship

$$\frac{\delta\langle r^2\rangle_{N_m,N2}}{\delta\langle r^2\rangle_{N_m,N1}}=\frac{\beta(Nm)-\beta(N2)}{\beta(Nm)-\beta(N1)}\ , \tag{19}$$

where Nm is a magic neutron number, $N2=Nm-4$, $N1=Nm-2$, and $\beta(N_i)$ is the binding energy per nucleon at the neutron number N_i. Starting from this correlation Gerstenkorn[41] takes

$$\delta\langle r^2\rangle_{Nm,\,Ni}\simeq -K[\beta(Nm)-\beta(N_i)]\ , \tag{20}$$

with $K>0$, and predicts negative isotope shifts for even isotopes approaching the magic neutron numbers 28, 50, and 82. In particular, he predicts $\langle r^2\rangle_{44}>\langle r^2\rangle_{46}\simeq\langle r^2\rangle_{48}$ for the calcium isotopes.

He also predicts $\langle r^2\rangle_{40}>\langle r^2\rangle_{48}$. This last prediction, although in accord with experiment, seems unwarranted, because if Eq. (19) is applied to the three isotopes Ca 40, Ca 44, and Ca 48, we are led to the conclusion that $\langle r^2\rangle_{40}>\langle r^2\rangle_{44}$—contrary to the experimental evidence. However, if we take $N2=Nm+4$ and $N1=Nm+2$, and apply Eq. (19) to the isotopes Ca 40, Ca 42, and Ca 44, we get

$$[\beta(40)-\beta(44)]/[\beta(40)-\beta(42)]=1.64,$$

while the results of the optical-isotope-shift experiment (see Table II) give

$$\delta\langle r^2\rangle_{40,44}/\delta\langle r^2\rangle_{40,42}=1.6\ .$$

Moreover, if we write Eq. (20) as

$$\delta\langle r^2\rangle_{Nm,N_i}=\langle r^2\rangle_{Nm}-\langle r^2\rangle_{N_i}=K[\beta(Nm)-\beta(N_i)]\ , \tag{21}$$

with $K>0$, applying it first to Ca 40 and Ca 42 and then to Ca 40 and Ca 44 yields, in concert with the above result, the prediction $\langle r^2\rangle_{40}<\langle r^2\rangle_{42}<\langle r^2\rangle_{44}$—in agreement with experiment. Once again we note that we cannot push too far. Application of Eq. (21) to the pair Ca 40 and Ca 48 with $Nm=20$ gives the erroneous result $\langle r^2\rangle_{40}<\langle r^2\rangle_{48}$.

VII. CONCLUSIONS

Optical-isotope-shift measurements can give information on both mass-effect and field-effect shifts in the spectrum lines of light elements. However, although the separation can, in principle, be accomplished solely with data from the optical-isotope-shift experiment, the current attainable accuracy demands the use of muonic x-ray data, atomic K x-ray data, or that from electron-scattering experiments. For the even-even calcium isotopes, the ζ,χ plot is linear to within experimental error so that the separation technique described should be valid. The variation of rms radius obtained from the optical volume shifts so acquired agrees qualitatively with that deduced from muonic x-ray and electron-scattering experiments—thus indicating that the separation is valid. It is estimated that the uncertainty in the optical-isotope-shift measurements must be reduced to $\sim 10^{-5}$ cm^{-1} before Eq. (6) can be meaningfully used. The correlation, observed by Gerstenkorn, between the relative isotope shifts in atomic spectrum lines and the binding energy per nucleon in the vicinity of magic neutron numbers holds for the even-even calcium isotopes—both near $N=20$ and near $N=28$. The relationship seems, however, to be valid only within four neutron numbers of a magic neutron number.

ACKNOWLEDGMENTS

The separated isotopes were purchased from the Oak Ridge National Laboratories. We would like to thank Mrs. Sylvia Shure of the National Bureau of Standards, Washington, D. C., for help in typing the manuscript during the tenure there of G. L. Epstein as a NRC-NBS Postdoctoral Associate. We also thank Mrs. Gabriel Epstein for editing the manuscript and typing corrected pages.

*Work supported by the National Science Foundation.

†Now with NASA/Goddard Space Flight Center, Greenbelt, Md. Temporary address: NASA Spectrometer Group, Sacramento Peak Observatory, Sunspot, N. M.

[1]H. Kopfermann, *Nuclear Moments* (Academic, New York, 1958).

[2]P. Brix and H. Kopfermann, Nachr. Akad. Wiss. Göttingen, II Math.-Physik. Kl. 31, 17 (1947).

[3]H. L. Anderson, C. S. Johnson, E. P. Hincks, S. Raboy, and C. C. Trail, Phys. Rev. Letters 6, 261 (1963).

[4]J. A. Bjorkland, S. Raboy, C. C. Trail, R. D. Ehrlich, and R. J. Powers, Phys. Rev. 136, B341 (1964).

[5]R. D. Ehrlich, D. Fryberger, D. Jensen, C. Nissim-Sabat, R. J. Powers, and V. L. Telegdi, Phys. Rev. Letters 18, 959 (1967).

[6]R. A. Eisenstein, D. W. Madsen, H. Theissen, L. S. Cardman, and C. K. Bockelman, Phys. Rev. 188, 1815 (1969).

[7]E. W. Foster, Rept. Progr. Phys. 14, 288 (1951).

[8]D. J. Hughes and C. Eckart, Phys. Rev. 36, 694 (1930).

[9]Reference 7, p. 292.

[10]Reference 1, p. 168.

[11]A. R. Bodmer, Proc. Phys. Soc. (London) 66, 69 (1953).

[12]A. F. Golovin and A. R. Striganov, Usp. Fiz. Nauk 93, 111 (1967) [Sov. Phys. Usp. 10, 658 (1968)].

[13]A. R. Bodmer, Nucl. Phys. 9, 371 (1958).

[14]Reference 12, English transl. p. 668.

[15]R. Bruch, K. Heilig, D. Kaletta, A. Steudel, and

D. Wendlandt, J. Phys. (Paris), Suppl. No. 1, 30, C1-51-8 (1969).

[16]L. Wilets, in *Handbuch der Physik*, edited by S. Flügge (Springer, Berlin, 1958), Vol. 38, p. 96.

[17]M. A. Preston, *Physics of the Nucleus* (Addison-Wesley, Reading, Mass., 1962), Chap. 3, p. 39.

[18]Reference 17, Chap. 3, pp. 39–49.

[19]B. Hahn, R. Hofstadter, and D. G. Ravenhall, Phys. Rev. 105, 1353 (1957).

[20]R. B. Chesler and F. Boehm, Phys. Rev. 166, 1206 (1968).

[21]S. K. Bhattacherjee, F. Boehm, and P. Lee, Phys. Rev. Letters 20, 1295 (1968).

[22]S. K. Bhattacherjee, F. Boehm, and P. Lee, Phys. Rev. 188, 1919 (1969).

[23]R. B. Chesler, Ph. D. dissertation (California Institute of Technology, 1967) (unpublished).

[24]E. C. Seltzer, Phys. Rev. 188, 1916 (1969).

[25]K. W. Ford and J. G. Wills, Phys. Rev. 185, 1429 (1969); H. A. Bethe and J. W. Negele, Nucl. Phys. A117, 575 (1968).

[26]C. S. Wu, in *Proceedings of the Arnold Summerfeld Centennial Memorial Meeting and of the International Symposium on the Physics of One- and Two-Electron Atoms, Munich*, 1968 (North-Holland, Amsterdam, Netherlands, 1969), pp. 479–486.

[27]Reference 15, Figs. 1–7.

[28]A. R. Bodmer, Nucl. Phys. 21, 347 (1960).

[29]Reference 12, English transl. p. 670.

[30]A. Pery, Proc. Phys. Soc. (London) A57, 181 (1954).

[31]A. Chantrel, Ann. Phys. (Paris) 4, 965 (1959).

[32]S. P. Davis, Appl. Opt. 2, 727 (1963).

[33]M. F. Crawford and A. L. Schawlow, Phys. Rev. 76, 1310 (1949).

[34]G. Racah, Nature 129, 723 (1932).

[35]S. Goudsmit, Phys. Rev. 43, 636 (1933).

[36]E. Fermi and E. Segrè, Z. Physik 82, 729 (1933).

[37]B. F. Gibson and K. J. Van Oostrum, Nucl. Phys. A90, 159 (1967).

[38]Reference 15, p. 6.

[39]Reference 1, Chap. 5, pp. 183–188.

[40]S. Gerstenkorn, Compt. Rend. 268, 1636 (1969).

[41]S. Gerstenkorn (unpublished).

PHYSICAL REVIEW A VOLUME 4, NUMBER 2 AUGUST 1971

g_J Value for the Atomic Ground State of Fermium†

L. S. Goodman, H. Diamond, H. E. Stanton, and M. S. Fred
Argonne National Laboratory, Argonne, Illinois 60439
(Received 5 November 1970)

The atomic-beam magnetic-resonance method has been used to measure $g_J = 1.160\,52 \pm 0.000\,14$ for the atomic ground state of fermium I. An intermediate-coupling calculation with parameters extrapolated from lower actinides, and with corrections for diamagnetic and relativistic effects, yielded the value $g_J = 1.1606$. The agreement between the measured and calculated values of g_J establishes the fermium ground state as the $^3H_6$ level of the $5f^{12}7s^2$ configuration. The neutral fermium atoms were obtained by heating FmF_3 and its HoF_3 carrier in the presence of ZrC and tungsten.

I. INTRODUCTION

The electron structure of the 100th element, fermium, can be predicted, but no isotope of this element has been available in more than nanogram amounts for experimental examination. The atomic-beam magnetic-resonance technique,[1] adapted to the measurement of radioactivity,[2] allows measurement of atomic and nuclear properties of small samples of radioactive species. A new atomic-beam apparatus has been used with 3–30-mCi charges of 3.24-h ^{254}Fm to measure the magnetic moment of the atomic ground state of the neutral fermium atom.

The measured g_J agrees with that calculated from an intermediate-coupling model with the use of parameters extrapolated from lower actinides or obtained from Hartree-Fock calculations. This agreement confirms that the ground state is the $^3H_6$ state of the $5f^{12}7s^2$ configuration.

The requirement for rapid production of a beam of neutral fermium atoms led to the use of zirconium carbide as a reducing agent.

II. PRODUCTION OF FERMIUM

Samples of ^{253}Es (20.4-day half-life) were intermittently available in 0.3–10-μg quantities. These were irradiated in the 5×10^{15}-neutron cm^{-2} sec^{-1} flux of the HFIR reactor to produce 39.3-h ^{254m}Es. The latter decays principally to ^{254}Fm, which can be separated from the einsteinium by α-hydroxyisobutyrate elution from cation-exchange columns. Three or four charges of fermium were obtained from each irradiated batch of einsteinium.

Upon isolation of ^{254}Fm in aqueous solution, 1 mg of Ho carrier was added and the fluorides of holmium and fermium were precipitated. The precipitate was washed twice with acetone, dried under a heat lamp, transferred to a zirconium carbide crucible, and covered with tungsten powder.